This article was downloaded by:
On: *21 January 2011*
Access details: *Access Details: Free Access*
Publisher *Taylor & Francis*
Informa Ltd Registered in England and Wales Registered Number: 1072954 Registered office: Mortimer House, 37-41 Mortimer Street, London W1T 3JH, UK

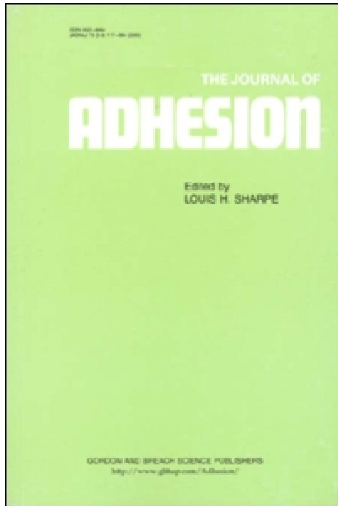

The Journal of Adhesion
Publication details, including instructions for authors and subscription information:
http://www.informaworld.com/smpp/title~content=t713453635

Modeling of Particle Removal using Non-contact Brush Scrubbing in Post-CMP Cleaning Processes

Reiyu Chein[a]; Wenyuan Liao[a]
[a] Department of Mechanical Engineering, National Chung Hsing University, Taichung, Taiwan

To cite this Article Chein, Reiyu and Liao, Wenyuan(2006) 'Modeling of Particle Removal using Non-contact Brush Scrubbing in Post-CMP Cleaning Processes', The Journal of Adhesion, 82: 6, 555 — 575
To link to this Article: DOI: 10.1080/00218460600766566
URL: http://dx.doi.org/10.1080/00218460600766566

PLEASE SCROLL DOWN FOR ARTICLE

Full terms and conditions of use: http://www.informaworld.com/terms-and-conditions-of-access.pdf

This article may be used for research, teaching and private study purposes. Any substantial or systematic reproduction, re-distribution, re-selling, loan or sub-licensing, systematic supply or distribution in any form to anyone is expressly forbidden.

The publisher does not give any warranty express or implied or make any representation that the contents will be complete or accurate or up to date. The accuracy of any instructions, formulae and drug doses should be independently verified with primary sources. The publisher shall not be liable for any loss, actions, claims, proceedings, demand or costs or damages whatsoever or howsoever caused arising directly or indirectly in connection with or arising out of the use of this material.

The Journal of Adhesion, 82:555–575, 2006
Copyright © Taylor & Francis Group, LLC
ISSN: 0021-8464 print/1545-5823 online
DOI: 10.1080/00218460600766566

Taylor & Francis
Taylor & Francis Group

Modeling of Particle Removal Using Non-contact Brush Scrubbing in Post-CMP Cleaning Processes

Reiyu Chein
Wenyuan Liao
Department of Mechanical Engineering, National Chung Hsing University, Taichung, Taiwan

Particle removal using non-contact brush scrubbing for post-CMP (Chemical Mechanical Planarization) cleaning is investigated analytically. The removal of SiO_2 and Al_2O_3 particles adhered onto SiO_2 film coated on the wafer surface are considered. The cleaning fluid ($H_2O/NH_4OH = 1{:}25$ and $1{:}200$) flowing between the brush and wafer surface is treated as a thin-film fluid flow. The flow field details and its effect on the drag force acting on the adhered particles are discussed. In addition to the drag force, the electrical double layer (EDL) and thermophoretic force effects on particle removal are also considered. It was found that the dominant force in achieving particle removal using a rolling mechanism is the drag force. The EDL and thermophoretic forces have an insignificant effect on particle removal. Based on the results from this study, particles of submicron size can be removed from a wafer surface using higher brush rotation speed and pure deionized (DI) water as the cleaning fluid.

Downloaded At: 20:41 21 January 2011

Keywords: Electrical double layer force; Particle rolling; Post-CMP cleaning; Thermophoretic force; Thin-film fluid flow

1. INTRODUCTION

With the high-speed development of Ultra Large Scale Integration (ULSI), the surface quality of a polished wafer surface on the produced device quality and yield rate is crucial. Chemical mechanical planarization (CMP), a surface preparation process for planarizing partially-processed silicon wafers in integrated circuit fabrications is at present the only process that can produce the required local and global

Received 5 December 2005; in final form 22 March 2006.
Address correspondence to Reiyu Chein, Department of Mechanical Engineering, National Chung Hsing University, 250 Kuo-Kuang Road, Taichung City, Taiwan 402. E-mail: rychein@dragon.nchu.edu.tw

planarity for multilevel interconnects in ULSI devices. Because CMP introduces foreign particles, metal contaminants and chemicals, it is referred as a dirty process. Post-CMP wafer cleaning has become an important step in successful CMP processes.

The currently used post-CMP cleaning techniques include brush scrubbing [1–3], ultrasonic and megasonic cleaning [4], fluid jet cleaning [5], laser heating [6] and chemical dissolution [7]. All of these techniques have practical limitations. Brush scrubbing is constrained by the size of the particles to be removed as the brush must establish good mechanical contact with the particles. Scratch damage could occur during the cleaning process. In the ultrasonic and megasonic cleaning processes, force produced by the sonic excitation should overcome the viscous effects and capillary force. Surface damage due to fluid cavitation could occur during high frequency excitation. Wet cleaning techniques such as jet impinging must be followed by a heating process. Local liquid vaporization and the generation of undesired chemicals might lead to wafer surface damage. In laser heating, a laser light is directly impinged onto the wafer surface causing both particle and surface expansion. The particles are removed by the thermal force from the material expansion. However, surface heating might create damage to the electrical circuits. The circuit damage limitation is the major concern in all of the particle cleaning techniques described above. The other major concern is the size of particles to be removed. As the device feature size continues to shrink, a cleaning technique capable of removing nanoscale particle sizes that prevents surface damage is critical. Advanced cleaning techniques such as shock wave [8] and plasma cleaning [9] have recently been proposed for non-contact nanosize particle cleaning.

Although brush scrubbing is limited by its capability to remove small particles, it is still the most frequently used technique in post-CMP cleaning because of its simplicity. Theoretically, effective particle removal can be achieved by raising the hydrodynamic force acting parallel on the particle and forces acting in the direction opposite to the adhesion force. The aims of this study are to improve the fluid flow model that describes cleaning fluid during non-contact brush scrubbing and examine the forces acting on the particle removal mechanisms. The flow field between the brush and wafer surface created by brush rotation is formulated by thin-film flow discussed in lubrication theory. The resulting velocity is then used to evaluate the hydrodynamic forces acting on the particles. Two forces are considered as acting vertically on the particles: the electrical double layer (EDL) and thermophoretic forces. The EDL force is due to the ionic concentration in the cleaning fluid and zeta potential interaction between the

Downloaded At: 20:41 21 January 2011

particle and wafer surface [10]. The thermophoretic force is due to the temperature gradient in the flow field [11].

2. MODEL

The schematic of non-contact brush scrubbing particle removal mechanism is shown in Fig 1. A brush has the radius of R_b rotating with an angular speed ω. Brush and wafer surface are separated by a small distance, h_0. Cleaning fluid is introduced into the gap between brush and wafer by brush rotation. A detailed schematic diagram of particle adhering to surface and forces acting on the particle is shown in Fig. 2. The particle has radius of R, adherent to the surface through a circular contact area of radius, r, and penetration distance, α. The particle is held on the surface by the adhesion force, F_a, which is acting vertically downward on the particle. As the brush rotates, the induced cleaning fluid flow produces drag force, F_D, and lift force, F_L, acting on the particle. In this study, the sum of all the forces having directions opposite to the adhesion force is denoted as the repulsive force, F_{rep}. Depending on the magnitudes of these forces, removing the particle from the surface can be achieved either by direct lift, sliding, or rolling [12]. Therefore, detailed examinations of the forces acting on the particle are important in modeling the cleaning process.

Downloaded At: 20:41 21 January 2011

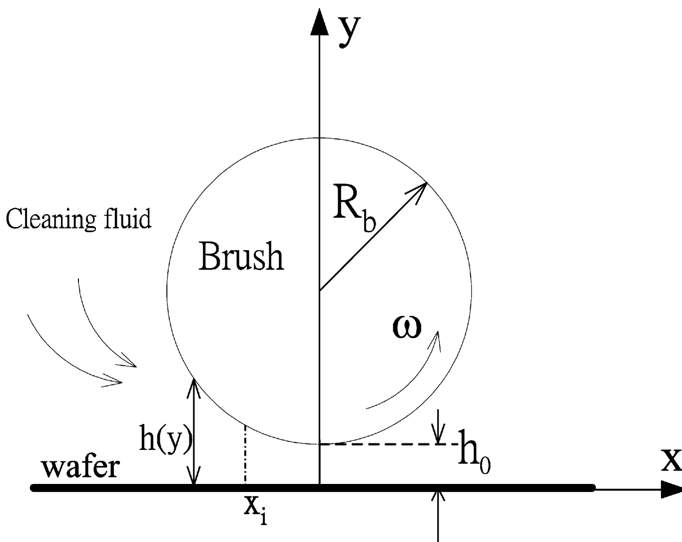

FIGURE 1 Schematic of non-contact brush scrubbing particle removing process.

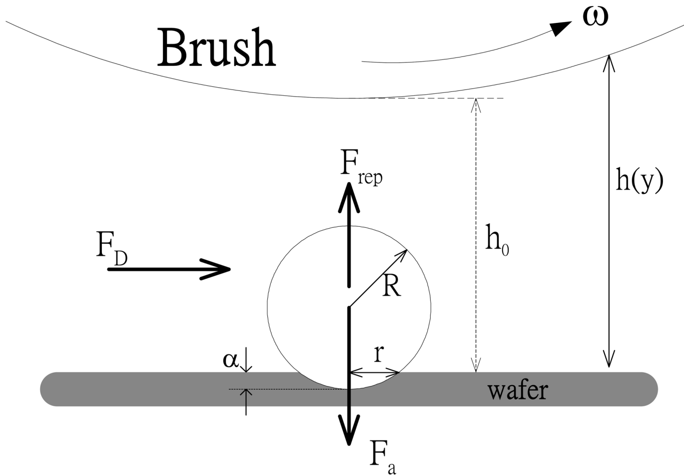

FIGURE 2 Schematic of forces acting on particle adherent on wafer surface during brush scrubbing cleaning process.

Downloaded At: 20:41 21 January 2011

2.1. Adhesive Force

For a particle immersed entirely in the fluid, the dominant adhesion force of small particles on a surface is due to the van der Waals force. The adhesion force for a spherical particle on a flat surface with a certain deformation at the particle-substrate interface is given as [10]:

$$F_a = \frac{A}{6Z_0^2}\left(R + \frac{r^2}{Z_0}\right), \tag{1}$$

where A, Z_0, and r are the Hamaker constant, separation distance between particle and surface and radius of contact area, respectively. The value of the Hamaker constant depends on the materials of the particle and wafer surfaces and the surrounding fluid medium. The value of Z_0 is usually taken as 0.2 nm for van der Waals bonded crystals [13]. The radius of the contact area is evaluated according to the JKR theory for a smooth surface without applied external force [14]:

$$r^3 = \frac{6\gamma\pi R^2}{K}, \tag{2}$$

where γ is the surface energy of adhesion depending on the materials of the particle and wafer surfaces. K is the composite

Young's modulus given by

$$K = \frac{4}{3}\left[\frac{(1-\nu_p^2)}{E_p} + \frac{(1-\nu_s^2)}{E_s}\right]^{-1}. \tag{3}$$

E_p and E_s are the values for Young's modulus. ν_p and ν_s are the Poisson's ratio values for the particle and surface, respectively. The penetration distance, α, can be computed from the geometric relation

$$\alpha = R - \sqrt{R^2 - r^2}. \tag{4}$$

2.2. Drag Force

For spherical particles in contact with a plane wall, O'Neill [15] proposed that the drag force acting on the particle due to the fluid flow could be calculated as

$$F_D = 1.7009 \times 6\pi\mu R u(R), \tag{5}$$

Downloaded At: 20:41 21 January 2011

where μ is the cleaning fluid viscosity, $u(R)$ is the fluid streamwise velocity component evaluated at a distance R from the plane wall. The velocity profile between the substrate surface and the brush surface is usually assumed to be linear for simplicity [1–3]. However, the flow field comprised by the substrate and brush actually form a thin layer fluid flow because the brush usually is located very close to the wafer surface to generate a larger drag force. In this situation, a pressure gradient would develop and the velocity would differ from a linear distribution in the thin-layer fluid flow. In this study, the thin-film flow described in lubrication theory is employed to describe the flow field between the brush and surface [16]. Based on the Reynolds equation given in lubrication theory, the pressure gradient in a thin-film flow created by brush rotation can be written as

$$\frac{d}{dx}\left(\frac{h^3}{12\mu}\frac{dP}{dx}\right) = \frac{U}{2}\frac{dh}{dx}. \tag{6}$$

In Eq. (6), h is the liquid film thickness, U is the brush tip velocity given as

$$U = R_b \frac{N}{60} 2\pi, \tag{7}$$

where N is the brush rotation speed in rpm. Referring to Fig. 1, since $x \ll R_b$ in the thin film region, h can be approximated by

$$h = h_0 + \frac{x^2}{2R_b}. \tag{8}$$

In Eq. (8), h_0 is the minimum liquid film thickness equal to the separation distance between the brush tip and wafer surface.

By integrating Eq. (6) twice, the pressure distribution in the thin film flow can be written as

$$P = 6\mu U\left[\frac{R_b x}{h_0(x^2+2h_0R_b)} + \frac{\sqrt{R_b}\tan^{-1}\left(\frac{x}{\sqrt{2h_0R_b}}\right)}{\sqrt{2}h_0^{3/2}}\right] + 12\mu C_1\left[\frac{xR_b^2}{h_0(x^2+2h_0R_b)^2} + \frac{3xR_b}{4h_0^2(x^2+2h_0R_b)} + \frac{3\sqrt{R_b}\tan^{-1}\left(\frac{x}{\sqrt{2h_0R_b}}\right)}{4\sqrt{2}h_0^{5/2}}\right] + C_2, \quad (9)$$

where C_1 and C_2 are the integration constants to be determined from the boundary conditions. The inlet location, x_i, where the fluid enters the gap between the bush and wafer surface, is assumed to be $-0.4R_b$ [17]. At the inlet, the liquid pressure is equal to the atmospheric pressure with a value of zero. For high brush rotation, the liquid film might be ruptured due to the fluid inertia effect [18]. To account for the film rupture effect on the pressure distribution, the film rupture model proposed by Swift and Stieber is used in this study [19]:

$$\frac{dP}{dx}\bigg|_{x=x_r} = P\bigg|_{x=x_r} = 0, \quad (10)$$

where x_r is the location where the film rupture occurs. The values for C_1, C_2, and x_r depend on the brush rotation speed and film thickness. They are determined iteratively from Eqs. (9) and (10).

The thin-film flow velocity can be obtained by solving the Navier-Stokes equations using the pressure distribution given in Eq. (9). To simplify this analysis, we neglect the fluid inertia effect on the velocity distribution. The resultant velocity distribution is

$$u = \frac{y}{h}U + \frac{1}{2\mu}\frac{dP}{dx}(y^2 - yh). \quad (11)$$

Note that the velocity profile depends on the location along the wafer surface and the classic Couette flow solution (linear velocity profiles) is regained if the pressure gradient is absent.

Downloaded At: 20:41 21 January 2011

2.3. Repulsive Force

Several repulsive forces could be possible during particle removal in the post-CMP process. In this study, we consider three possible repulsive forces: the electrical double layer repulsive force, thermophoretic force and hydrodynamic lift force.

2.4. Electrical Double Layer Repulsive Force

The electrical double layer forces are associated with particles whose effective diameters are smaller than 5 μm [10]. A surface contact potential is created between two different materials based on each material's respective local energy state. The resulting surface charge build-up needed to preserve charge neutrality sets up a double layer charge region, thus, creating an electrical attraction or repulsion force known as the electrical double layer (EDL) force.

An approximate analytical solution for the EDL interaction potential between spheres, called the HHF formula, was derived by Hogg *et al.* [20]. The HHF formula can be extended to the interaction between a sphere and plane surface by letting the radius of one of the spheres be equal to infinity [21]. By taking the derivative of the EDL interaction potential between a particle and wall with respect to the separation distance, the EDL force can be expressed as

$$F_{edl} = \frac{k_b T}{R} E_1 \tau \left[\frac{e^{-\tau D}}{1 + e^{-\tau D}} - E_2 \frac{e^{-2\tau D}}{1 - e^{-2\tau D}} \right], \tag{12}$$

where $k_b = 1.381 \times 10^{-23}$ J/K is the Boltzmann constant, T is the absolute fluid temperature and D is the ratio of separation distance to the particle radius. In post-CMP cleaning, D is given as Z_0/R. The parameters E_1, E_2, and τ appearing in Eq. (12) are the EDL parameter, EDL asymmetrical parameter, and reduced particle radius, respectively. They are defined as

$$E_1 = \frac{4\pi \varepsilon_r \varepsilon_0 R \zeta_p \zeta_s}{k_b T}, \tag{13a}$$

$$E_2 = \frac{(\zeta_p - \zeta_s)^2}{2\zeta_p \zeta_s}, \tag{13b}$$

and

$$\tau = \frac{R}{k^{-1}} = kR, \tag{13c}$$

where ζ_p and ζ_s are the zeta potentials of the particle and surface, respectively. ε_r is the relative dielectric permittivity of the fluid

Downloaded At: 20:41 21 January 2011

medium and $\varepsilon_0 = 8.85 \times 10^{-12}$ C/V·m is the permittivity of a vacuum. k^{-1} is the Debye length or the EDL thickness determined by the ion concentration in the fluid medium. Based on Eq. (12), the EDL force depends on the particle size, separation distance, Debye length and zeta potential of the particle and wall. As mentioned by Hogg *et al.* [20], Eq. (12) should be a good approximation for determining the EDL interaction between a sphere and a flat plate as $|\zeta_p|$ and/or $|\zeta_s| < 60$ mV and $\tau > 5$. Moreover, the repulsive electrical force can result only when both ζ_p and ζ_s have the same sign (positive or negative), as indicated in Eq. (12).

2.5. Theromophoretic Force

When a temperature gradient is present in a flow field, the particle experiences thermophoretic force in addition to drag, lift and the EDL forces. In the post-CMP cleaning process, a temperature gradient in the flow field can be generated by heating the wafer slightly. The resultant thermophoretic force has opposite direction to the adhesion force and, therefore, helps particle removal. In the past, many studies focused on the thermophoretic force on a particle suspended in a gas flow field. This theory has been well established [11]. Relatively few studies have addressed the thermophoretic force on a particle suspended in a liquid flow. In this study, the model for a thermophoretic force acting on a particle suspended in a liquid can be expressed as

$$F_{Th} = 6\pi\mu\nu R k_{th} \frac{\nabla T}{T}, \tag{14}$$

where k_{th} is the thermophoretic coefficient for a particle suspended in a liquid given by McNab and Meisen [22]:

$$k_{th} = -0.26 \frac{k_f}{2k_f + k_p}. \tag{15}$$

The theromphoretic force is proportional to the particle size and temperature gradient in the flow field.

2.6. Lift Force

The expression predicting the lift force acting on a sphere in the region near an infinite plate is given by Cherukat *et al.* [23]:

$$F_L = 9.22 R^2 u(R)^2. \tag{16}$$

F_L is expected to be small since it depends on the square of the particle size.

Downloaded At: 20:41 21 January 2011

3. RESULTS AND DISCUSSION

The above established cleaning mechanism and force models were used to evaluate non-contact brush scrubbing particle cleaning. Several parameters must be specified in advance. The brush radius is taken as 2.85 cm and its temperature is kept at 20°C [1]. The particle radius range to be studied is from 0.1 to 1 μm. The cleaning fluid is a diluted ammonium hydroxide ($NH_4OH + H_2O$) alkaline aqueous solution. The NH_4OH concentration is in the range of 0.5 to 4% [24]. The thermophysical properties of the cleaning fluid are assumed identical with DI water. Two types of particles, SiO_2 and Al_2O_3, adhered on a wafer surface coated with a thin SiO_2 layer are considered in this study. During cleaning the wafer is assumed to be heated to a temperature of 80°C.

Downloaded At: 20:41 21 January 2011

3.1. Pressure and Velocity in the Thin Film Flow Between the Brush and Wafer

To evaluate the drag force acting on the particle, the pressure distribution and flow velocity must be solved in advance. Typical pressure distribution along the wafer surface is shown in Fig. 3 for N = 100 and 300 RPM. The $h_0 = 3\,\mu m$ and $10\,\mu m$ values are used in the computations in Fig. 3. The pressure increases along the wafer surface and reaches a maximum value P_{max} at a location x_{max}. After reaching the maximum value, the pressure drops sharply to zero at the film rupture location x_r. The maximum pressure, maximum pressure location, film rupture location and constants C_1 and C_2 values in Fig. 3 are tabulated in Table 1. In general, the maximum pressure magnitude increases with the increase in N and decreases with the decrease in h_0.

The pressure distribution shown in Fig. 3 indicates that there is an adverse pressure gradient in the $x_i < x < x_{max}$ region while a favorable pressure gradient exits in the $x_{max} < x < x_r$ region. From fluid mechanics, it is expected that a reversed flow exists due to an adverse pressure gradient and accelerated flow due to the favorable pressure gradient in the near-wall region. Fig. 4 shows the typical velocity profiles along the wafer surface for N = 100 RPM and $h_0 = 3\,\mu m$. The reversed flows are clearly seen at $x = -0.1R_b$ and $-0.013R_b$. For particles adhered in the adverse pressure gradient region, a particle might be removed in the negative x direction because of the drag force direction. However, this might be difficult because the velocity magnitude in the reversed flow region is generally small and, consequently, the drag force is weak. Therefore, the greatest particle removal potential occurs in the $x_{max} < x < x_r$ region where stronger drag force occurs

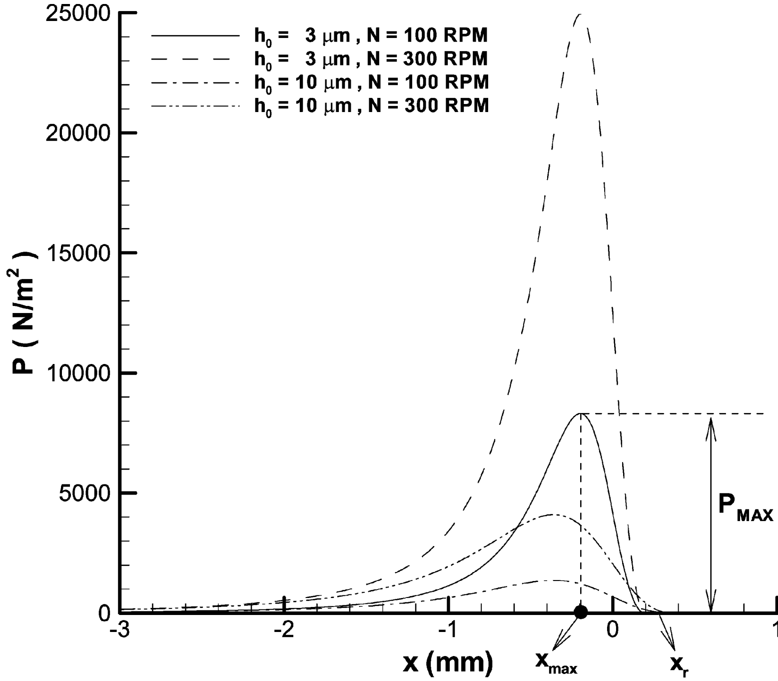

FIGURE 3 Pressure distribution of thin-film fluid flow between brush and wafer surface.

Downloaded At: 20:41 21 January 2011

in the positive x direction due to the favorable pressure gradient. Note that the linear velocity profile occurs at $x_{\max}$ instead of x = 0 because the pressure gradient is zero at $x_{\max}$.

3.2. Force Acting on Particles

The forces acting on the particle can be computed based on the obtained velocity distribution and force models described above.

TABLE 1 Summary of Pressure Distribution Results (Fig. 3)

h_0 (μm)	N (RPM)	$P_{\max}$ (N/m^2)	$x_{\max}$ (m)	x_r (m)	C_1	C_2
3	100	8315.09	-0.1938×10^{-3}	0.19647×10^{-3}	-0.548733×10^{-6}	4157.9
	300	24945.3	-0.1938×10^{-3}	0.19647×10^{-3}	-0.16462×10^{-5}	12473.7
10	100	1365.6	-0.3534×10^{-3}	0.358638×10^{-3}	-0.182899×10^{-5}	682.865
	300	4096.79	-0.3534×10^{-3}	0.358638×10^{-3}	-0.548696×10^{-5}	2048.6

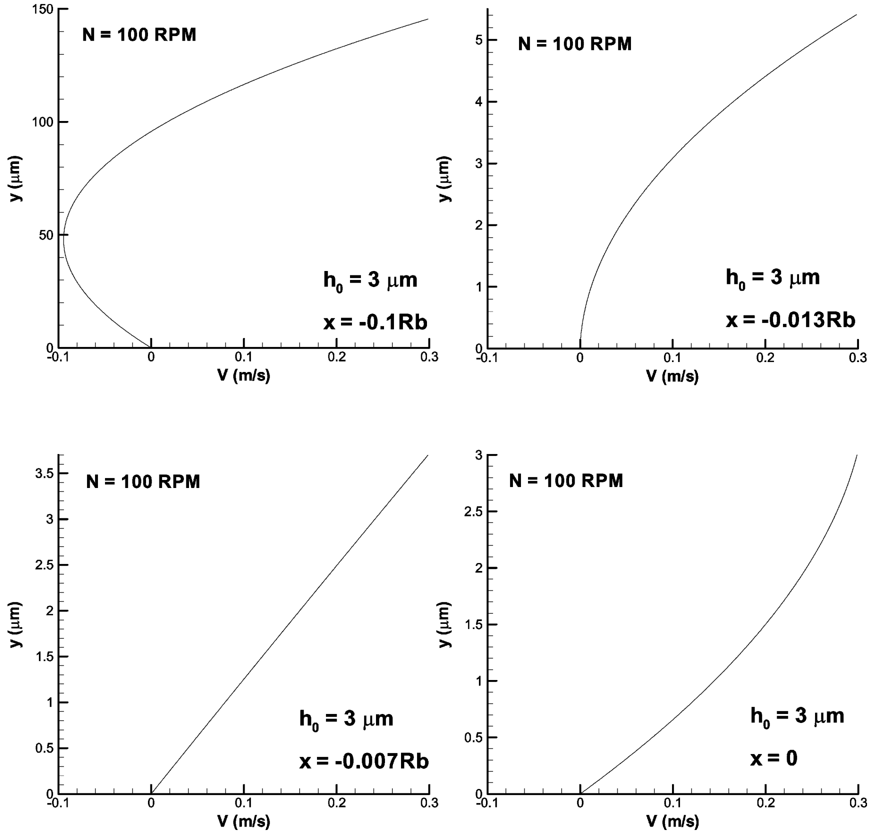

FIGURE 4 Velocity profiles along the wafer surface during brush scrubbing.

Downloaded At: 20:41 21 January 2011

Without losing the generality, we consider only the particles adhered at x = 0. In Fig. 5, the forces acting on a SiO_2 particle adhered on the SiO_2 surface as a function of the particle radius are shown for N = 100 RPM and $h_0 = 3\,\mu m$. The adhesive force is computed from Eq. (1) using the material properties listed in Table 2. The drag force is evaluated from Eq. (5) using the velocity distribution described in Eq. (11). The ζ_p, ζ_s and k^{-1} values are needed in evaluating the EDL force. These values are listed in Table 3 for NH_4OH with concentrations of 0.5% and 4% in a water solution [25]. The thermophoretic force is computed from Eq. (14). Note that the temperature gradient depends on h_0 and the temperature difference between the brush and wafer. As shown in Fig 5, all forces increase with the increase in particle radius. As expected, the adhesive force is the strongest of

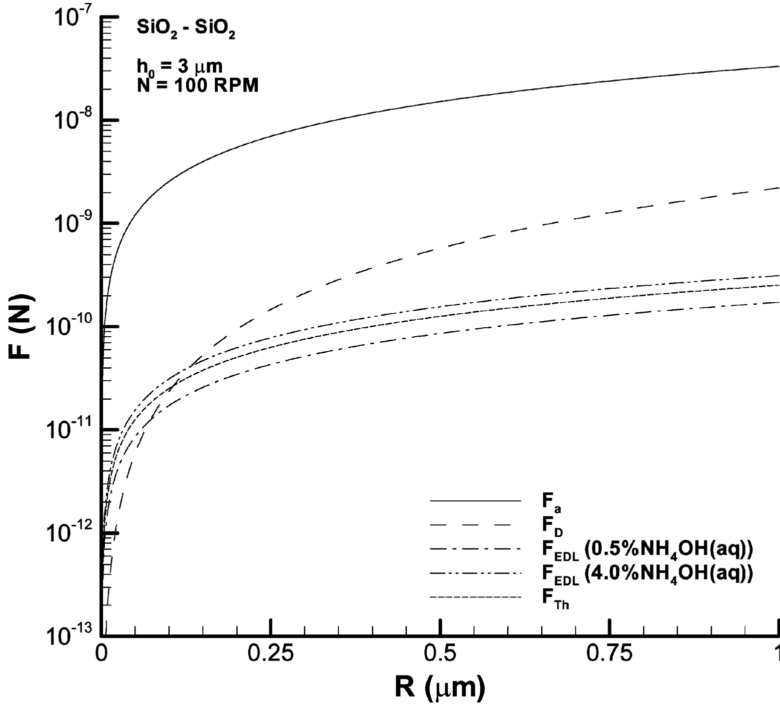

FIGURE 5 Forces acting on SiO_2 particle adherent on SiO_2 thin film. $h_0 = 3\,\mu\text{m}$.

Downloaded At: 20:41 21 January 2011

TABLE 2 Material Properties Used in Computing Forces

Property name	SiO_2	Al_2O_3	H_2O	$SiO_2 - H_2O - SiO_2$	$Al_2O_3 - H_2O - SiO_2$
Hamaker constant $A \times 10^{-20}$ (J)	8.8	16.75	4.0	1.8	3.58e
Surface energy with SiO_2 film, $\gamma \times 10^{-2}$ (J/m^2)				1.459	1.913
Young's modulus(GPa)	73	400			
Poisson ratio	0.17	0.27			
Thermal conductivity (W/mK)	1.4	30	0.6		

TABLE 3 EDL Parameters Used in Computing EDL Force

	0.5% NH_4OH aqueous solution		4% NH_4OH aqueous solution	
pH	9.75		10.23	
k^{-1} (nm)	42.4		23.3	
ζ_p (mV)	SiO_2	−41	SiO_2	−41
	Al_2O_3	−45	Al_2O_3	−56
ζ_s (mV)	SiO_2	−41	SiO_2	−41

these forces. The repulsive EDL forces between a SiO_2 particle and SiO_2 surface are obtained for both NH_4OH concentrations studied. The EDL force is seen to increase with the increase in NH_4OH concentration. From Fig. 5, the thermophoretic force can be greater than the EDL force when $h_0 = 3\,\mu m$.

By increasing h_0 to 10 μm and keeping N = 100 RPM, the forces acting on the SiO_2 particle are shown in Fig. 6. The drag force is reduced

Downloaded At: 20:41 21 January 2011

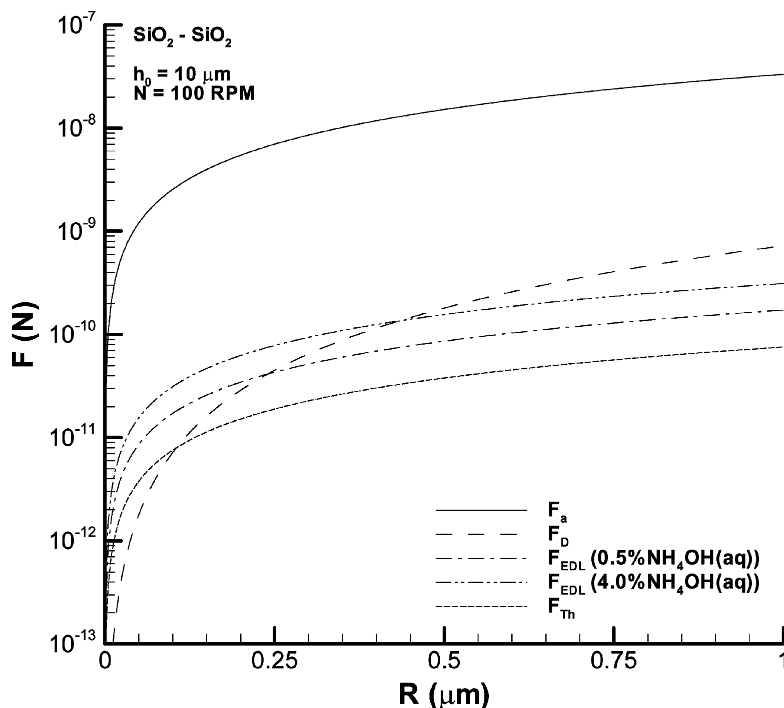

FIGURE 6 Forces acting on SiO_2 particle adherent on SiO_2 thin film. $h_0 = 10\,\mu m$.

due to the enlarged flow passage. The EDL forces remain the same as those in Fig. 5 because they are independent of N and h_0. The thermophoretic force is also reduced because of the decrease in temperature gradient.

The forces acting on an Al_2O_3 particle adhered onto the SiO_2 surface can be computed in the same way as that for Figs. 5 and 6. The results are shown in Figs. 7 and 8. Because the drag force depends on N, h_0, and the particle radius, the drag force acting on Al_2O_3 particles have the same values as those shown in Figs 5 and 6 under the same N, h_0, and particle radius range. However, the EDL and thermopohoretic forces are different from those in Figs. 5 and 6 because of the differences in zeta potential and the material properties. In Figs. 7 and 8, the EDL force becomes attractive when a 4%-NH_4OH water solution is used. By inspecting Eq. (12), it can be seen that the attractive EDL force is due to the asymmetrical EDL interaction. Therefore, removing Al_2O_3 particles is more difficult than SiO_2

Downloaded At: 20:41 21 January 2011

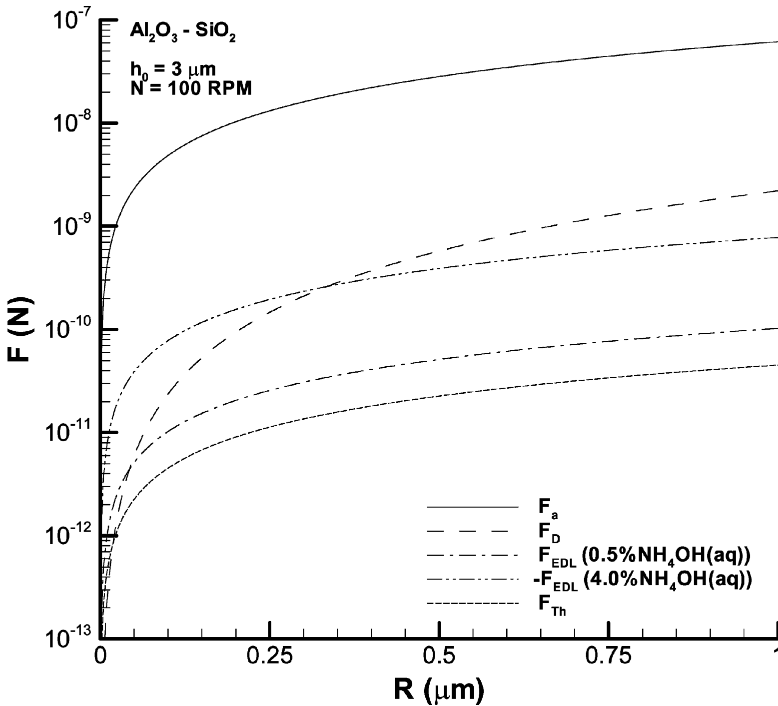

FIGURE 7 Forces acting on Al_2O_3 particle adherent on SiO_2 thin film. $h_0 = 3\,\mu m$.

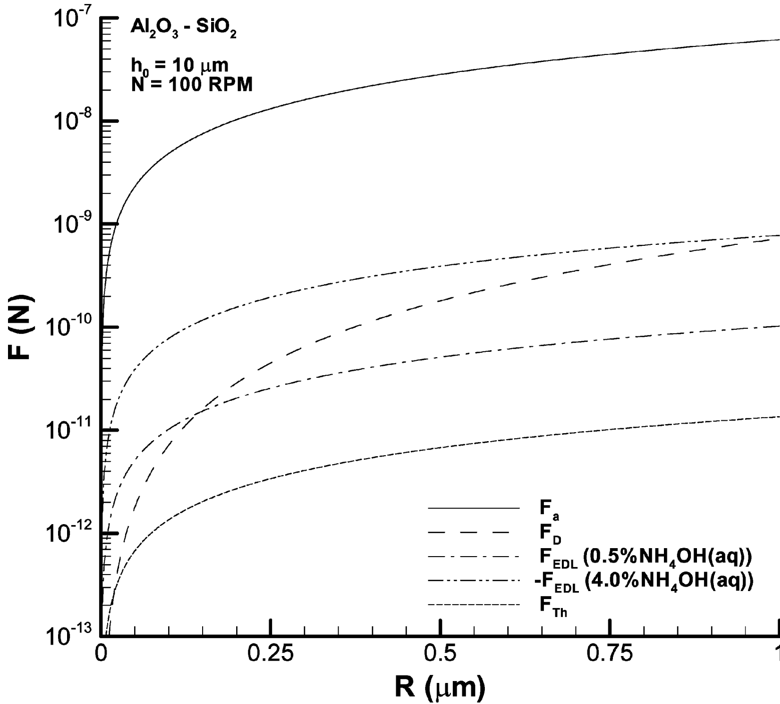

FIGURE 8 Forces acting on Al_2O_3 particle adherent on SiO_2 thin film. $h_0 = 10\,\mu\text{m}$.

Downloaded At: 20:41 21 January 2011

particles when the cleaning fluid contains high concentrations of NH_4OH.

The lift force produced by the fluid flow can be computed from Eq. (16). For the particle radius range studied, the largest lift force is of the order 10^{-15} N which is relatively smaller compared with the other forces. The lift force is then neglected in the following discussion on the particle removing mechanism.

3.3. Particle Removal Mechanism

From the results shown in Figs. 5–8, the most possible particle removal mechanism is particles rolling to the positive x direction because both F_{rep} and F_D are less than F_a. The removal moment and adhesion resistant moment ratios, F_r, must be greater than 1, *i.e.*,

$$F_r = \frac{F_D(1.399R - \alpha) + rF_{rep}}{rF_a} > 1, \tag{17}$$

for the particles to roll. The factor 1.399 in Eq. (17) accounts for the nonuniformity of the flow field [15]. In Figs. 9 and 10, F_r as functions of the brush rotation speed and particle radius are shown for SiO_2 particles adhered to the SiO_2 surface with $h_0 = 3\,\mu m$ and $h_0 = 10\,\mu m$, respectively. The NH_4OH concentration is 4%. Since the drag force is related to N and h_0, the smallest particle size that can be removed decreases with the increase in N. For $h_0 = 3\,\mu m$ case, the smallest particle size that can be removed is about $0.1\,\mu m$ when N = 300 RPM. In the $h_0 = 10\,\mu m$ case, the smallest particle size that can be removed increases to $0.25\,\mu m$ because of the reduction in drag force.

Under the same operating conditions for Figs. 9 and 10, the moment ratio, F_r, for the Al_2O_3 particle adhered onto the SiO_2 surface can also be computed and the results are shown in Figs. 11 and 12. As noted earlier, the EDL force in the 4%-NH_4OH water solution becomes negative. Therefore, the smallest Al_2O_3 particle size that can be

Downloaded At: 20:41 21 January 2011

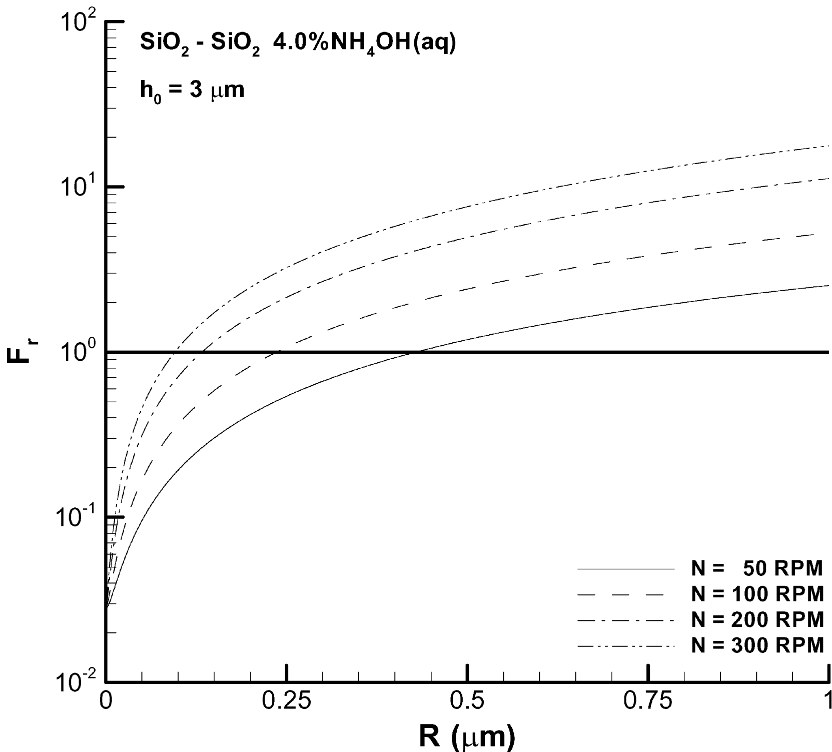

FIGURE 9 Particle removing moment as functions of brush rotation speed and particle size for SiO_2 particle adherent on SiO_2 thin film. $h_0 = 3\,\mu m$.

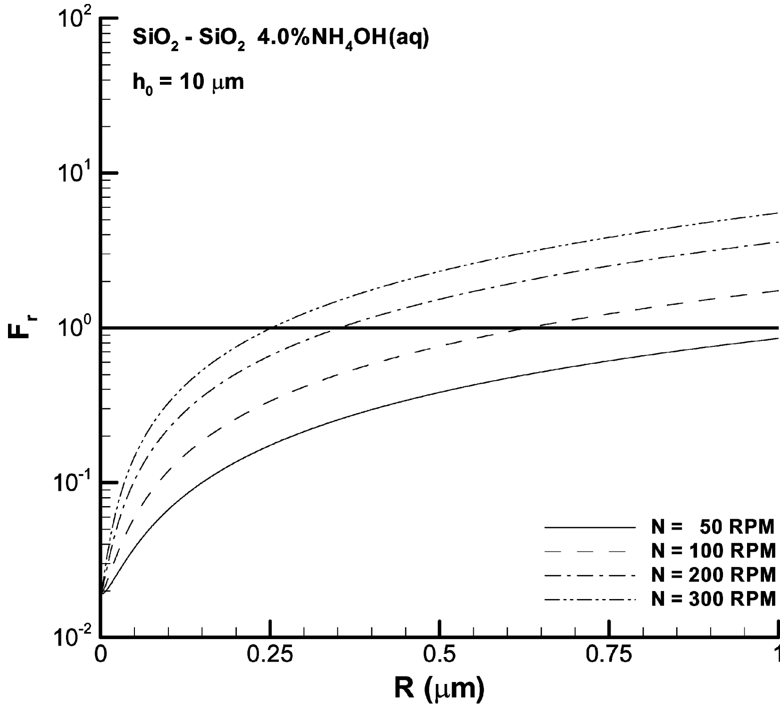

FIGURE 10 Particle removing moment as functions of brush rotation speed and particle size for SiO_2 particle adherent on SiO_2 thin film. $h_0 = 10\,\mu m$.

Downloaded At: 20:41 21 January 2011

removed under the same rotation speed is larger than that for SiO_2 particles. As shown in Fig. 11, the smallest particle size that can be removed is about $0.25\,\mu m$ when $h_0 = 3\,\mu m$ and $N = 300\,rpm$. For the $h_0 = 10\,\mu m$ and $N = 300\,rpm$ case shown in Fig. 12, the smallest particle size increases to $0.4\,\mu m$.

To show the repulsive force effect on particle removal, F_r as a function of the particle size with and without the repulsive force are compared. The typical results are shown in Fig. 13. The repulsive force actually does not help particle removal very much (see the inserts in Fig. 13). The main force causing particle removal by rolling is the drag force. The repulsive forces due to the EDL interaction and thermophoretic effect become effective in particle removal when their magnitudes can be raised to the same order as the drag force. This requires suitable cleaning agent concentration adjustment in the water solution and increasing the temperature difference between the wafer and brush. However, determining a suitable water cleaning agent

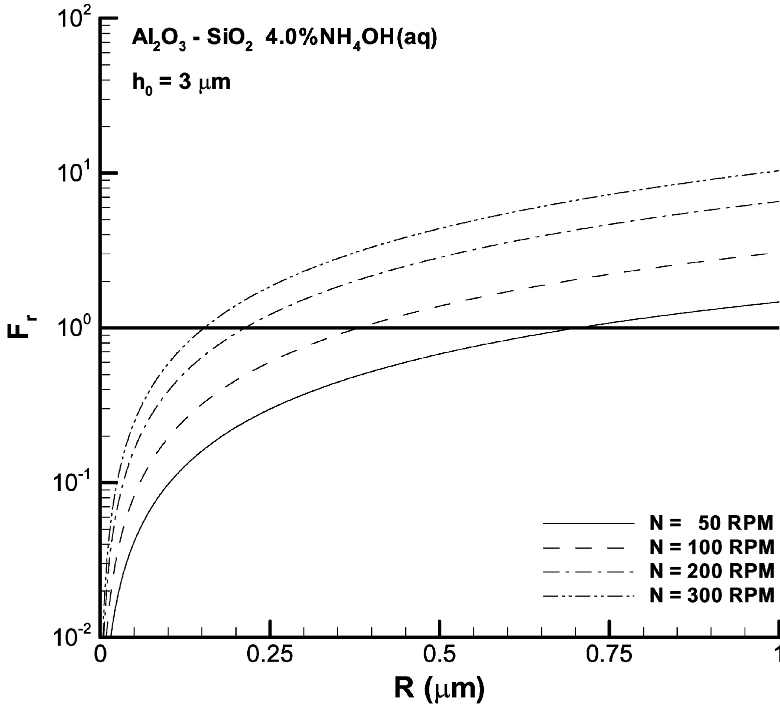

FIGURE 11 Particle removing moment as functions of brush rotation speed and particle size for Al_2O_3 particle adherent on SiO_2 thin film. $h_0 = 3\,\mu m$.

Downloaded At: 20:41 21 January 2011

solution combination is time consuming and the high temperature operation could damage the circuits. Based on the results obtained in this study, using pure DI water as the cleaning fluid and higher brush rotation speed in the post CMP cleaning process is adequate for removing particles less than $1\,\mu m$ in size.

4. CONCLUSION

A theoretical study on post-CMP particle removal using non-contact brush scrubbing was performed. In contrast to past studies, the fluid flow between the brush and wafer surface was modeled using the thin-layer fluid flow described in lubrication theory. The drag force acting on the particle was then computed using the modified fluid velocity. In addition to the drag force, the EDL and thermophoretic forces acting vertically on an adhered particle were analyzed in detail. Two types of particles, SiO_2 and Al_2O_3, adhered onto a SiO_2 layer coated

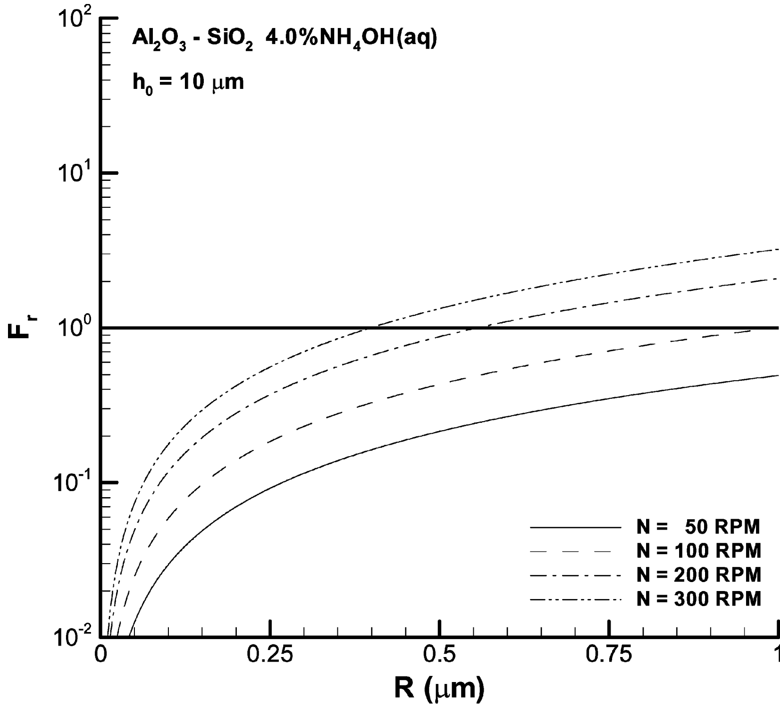

FIGURE 12 Particle removing moment as functions of brush rotation speed and particle size for Al_2O_3 particle adherent on SiO_2 thin film. $h_0 = 10\,\mu m$.

Downloaded At: 20:41 21 January 2011

on the wafer surface were considered. The cleaning fluid was a diluted ammonium hydroxide ($NH_4OH + H_2O$) alkaline aqueous solution.

The drag force depends on the brush rotation speed (N) and separation distance between the wafer surface and brush tip (h_0). The velocity profiles along the wafer surface are not linear except at the maximum pressure location. The EDL force was found to be repulsive for the SiO_2 particle-SiO_2 surface interaction for the two cleaning agent concentrations used. The EDL force becomes attractive in the Al_2O_3 particle-SiO_2 surface interaction when a high NH_4OH concentration is involved. This attractive EDL force makes the Al_2O_3 particle more difficult to remove from the wafer surface. The thermophoretic force is proportional to the temperature gradient in the flow field and can exceed the EDL force when the separation distance between the wafer and brush tip is small. Although the repulsive force can reduce the smallest particle size that can be removed under given N and h_0, the difference is not very significant. Suitable cleaning agent

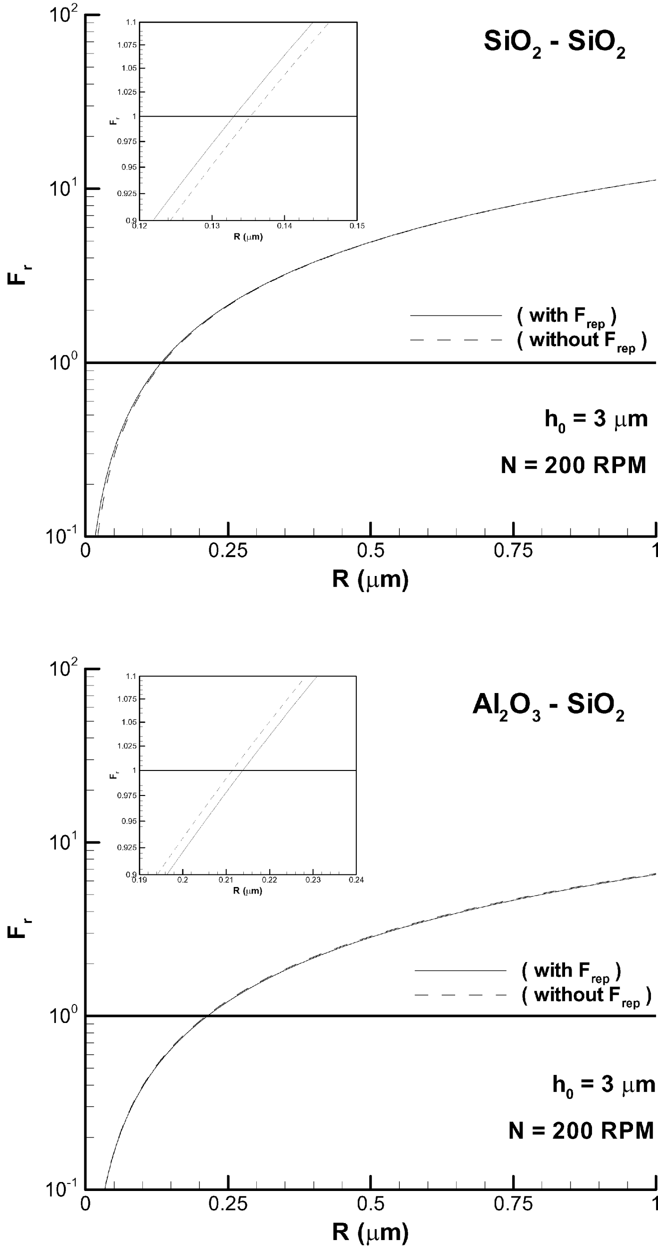

FIGURE 13 Comparisons of removing moments with and without including repulsive forces.

Downloaded At: 20:41 21 January 2011

concentration adjustment in the cleaning fluid and increasing the temperature gradient in the flow field could help reduce the smallest particle size that could be removed. However, this approach is time consuming and increases the possibility of circuit damage from heating. Based on the results from this study, it is suggested that pure DI water and higher brush rotation speed would be adequate in removing particles in the submicron size range.

REFERENCES

[1] Zhang, G., Burdick, G., Dai, F., Bibby, T., and Beaudoin, S., *Thin Solid Films* **332**, 379–384 (1998).
[2] Busnaina, A. A., Lin, H., Moumen, N., Feng, J., and Taylor, J., *IEEE Trans. On Semiconductor Manufacturing* **15**, 374–382 (2002).
[3] Roy, S. R., Ali, I., Shinn, G., Furusawa, N., Shah, R., Peterman, S., Witt, K., and Eastman, S., *J. Electrochem. Soc.* **142**, 216–226 (1995).
[4] Qi, Q. and Brereton, G. J., *IEEE Trans. On Ultrasonics, Ferroelectrics, and Frequency Control* **42**, 619–629 (1995).
[5] Otani, Y., Namiki, N., and Emi, H., *Aerosol Sci. Tech.* **23**, 665–673 (1995).
[6] Arnold, N., *Applied Surface Sci.* **208–209**, 15–22 (2003).
[7] Wang, Y. L., Liu, C., Feng, M. S., and Tseng, W. T., *Materials Chemistry and Physics* **52**, 23–30 (1998).
[8] Busnaina, A. A., Park, J. G., Lee, J. M., and You, S. Y., *In IEEE/SEMI Advanced Manufacturing Conference*, 41–45 (2003).
[9] Cetinkaya, C., Murthy, M. D., and Peri, P., *Nanotechnology* **15**, 435–440 (2004).
[10] Bowling, R. A., *J. Electrochem. Soc., Solid State Sci. Tech.* **132**, 2208–2214 (1985).
[11] Talbot, L., Cheng, R. K., Schefer, R. W., and Willis, D. R., *J. Fluid Mech.* **101**, 737–758 (1980).
[12] Wang, H., *Aerosol Sci. Tech.* **13**, 386–393 (1990).
[13] Israelachvili, J., *Intermolecular and Surface Forces* (Academic Press, New York, 1992), pp. 178–181.
[14] Johnson, K. L., Kendall, K. K., and Roberts, A. D., *Proc. Royal Soc. London Series A* **324**, 301–313 (1971).
[15] O'Neill, M. E., *Chem. Eng. Sci.* **23**, 1293–1298 (1968).
[16] Hamrock, B. J., *Fundamentals of Fluid Film Lubrication* (McGraw-Hill, New York, 1994), pp. 161–167.
[17] You, H. I. and Lu, S. S., *ASME J. Tribology* **109**, 87–90 (1987).
[18] Malvano, R. and Vatta, F., *ASME J. Lubrication Tech.* **105**, 77–83 (1983).
[19] Schumack, M. R., Chung, J. B., Schultz, W. W., and Kannatey-Asibu, E., *ASME J. Eng. Ind.* **113**, 190–197 (1991).
[20] Hogg, R., Healy, T., and Fuerstenau, D. W., *Trans. Faraday Soc.* **62**, 1638–1651 (1966).
[21] Yang, C., Dabros, T., Li, D., Czarnecki, J., and Masliyah, J. H., *J. Colloid Interface Sci.* **208**, 226–240 (1998).
[22] McNab, G. S. and Meisen, A., *J. Colloid Interface Sci.* **44**, 339–346 (1973).
[23] Cherukat, P. and McLaughlin, J. B., *J. Fluid Mech.* **23**, 1–18 (1994).
[24] Pan, T., Lei, T., Chen, C., Chao, T., Liaw, M., Yang, W., Tsai, M., Lu, C. P., and Chang, W., *IEEE Electron Device Letters* **21**, 338–340 (2000).
[25] Tardif, F., Constant, I., Lardin, T., Demolliens, O., Fayolle, M., Gobil, Y., Palleau, J., and Torres, J., *Microelectronic Eng.* **37/38**, 285–291 (1997).

Downloaded At: 20:41 21 January 2011